

Topologically enhanced localization and optical switching in the one-dimensional periodically driven Shockley model

Yiqi Zhang,^{1,2, a)} Da Zhang,¹ Zhaoyang Zhang,^{1,2} Yanpeng Zhang,^{1, b)} Milivoj R. Belić,³ and Min Xiao^{4,5}

¹⁾Key Laboratory for Physical Electronics and Devices of the Ministry of Education & Shaanxi Key Lab of Information Photonic Technique, Xi'an Jiaotong University, Xi'an 710049, China

²⁾Department of Applied Physics, School of Science, Xi'an Jiaotong University, Xi'an 710049, China

³⁾Science Program, Texas A&M University at Qatar, P.O. Box 23874 Doha, Qatar

⁴⁾Department of Physics, University of Arkansas, Fayetteville, Arkansas 72701, USA

⁵⁾National Laboratory of Solid State Microstructures and School of Physics, Nanjing University, Nanjing 210093, China

(Dated: 3 December 2024)

We investigate topologically enhanced localization and optical switching in the one-dimensional (1D) periodically driven Shockley model, theoretically and numerically. Transport properties of the model, arranged as a 1D photonic array of waveguides, are discussed. We find that light beam propagating in such an array can be well localized under both periodic and open boundary conditions, thanks to the zero-energy and edge states that depend on the topological structure of quasi-energy. Topological protection of the localization due to the edge state is demonstrated, based on which an optical switch with high efficiency is proposed.

PACS numbers: 03.65.Vf, 42.25.Gy, 78.67.-n

Over recent years, periodically driven systems have attracted much attention in condensed matter physics¹⁻⁹ and photonics¹⁰⁻¹⁵. It has been demonstrated that the periodic driving mechanism breaks the time-reversal symmetry and leads to the topological phase transition in the system. One remarkable feature is the appearance of edge states, which are topologically protected and immune to defects. In photonics, such a mechanism plays the role of “magnetic field” or spin-orbit coupling for photons, which helped in the development of photonic interconnects, delay lines, isolators, couplers, and other photonic devices¹⁶.

According to the Floquet theory, the Hamiltonian of a periodically driven system satisfies the condition $H(t) = H(t + T)$, where T is the period of the driving “force”. In a periodically driven system, the propagation of light is described by an evolution operator $U(t) = \mathcal{T} \exp[-i \int_0^t H(\mathbf{k}, t') dt']$, where \mathcal{T} is the time-ordering operator and \mathbf{k} the momentum. Over one period, the bulk evolution operator is $U(T)$, which corresponds to an effective Hamiltonian H_{eff} through $U(T) = \exp(-iH_{\text{eff}}T)$. The effective Hamiltonian H_{eff} is time-independent, and allows a stroboscopic view of the propagation dynamics over the full period. The quasi-energy ϵ ^{17,18} corresponding to the system can be obtained from the expression $U(T)|\phi\rangle = \exp(-i\epsilon T)|\phi\rangle$, where $|\phi\rangle$ is the Floquet eigenstate. Based on this simple idea, photonic (anomalous) topological insulators were reported^{13,16}. The “anoma-

lous” meant that the number of edge states could not be predicted by the bulk-edge correspondence¹⁹, which is true for a static system but not for a periodically-driven system.

Concerning an edge state, it is chiral in two-dimensional (2D) periodically driven systems, which leads to the light propagating along the boundary of the system in a certain direction^{13,20-22}. Considering that previous investigations were mainly focused on 2D and 3D systems, we wondered what might happen in a one-dimensional periodically driven system. Hence the motivation for this study. One should bear in mind that if the edge state is constant throughout the first Brillouin zone, light will not propagate but will be localized on the boundary of the sample²³.

In this Letter, we consider a one-dimensional discrete system based on the Shockley model²⁴, as shown in Fig. 1(a), which is quite similar to the Su-Schrieffer-Heeger model²⁵, introduced in 1979. The system is composed of two distinct sites A and B in the unit cell of a 1D lattice, with alternating hopping strengths. In addition to the original model, we assume that the hopping strengths between the sites are periodic. In the first step, the hopping only happens on the right-hand side with the strength J_1 (we take site A as a reference), while in the second step, the hopping happens on the left-hand side, with the strength J_2 . For simplicity, we assume $J_1 = J_2 = J$. By adjusting the coupling strength J , we will show that the dispersion relation of this model under the periodic boundary condition could be linear or zero in the first Brillouin zone. However, under the open boundary condition, a topologically protected edge state will emerge gradually with increasing J , which indicates that the sys-

^{a)}zhangyiqi@mail.xjtu.edu.cn

^{b)}ypzhang@mail.xjtu.edu.cn

tem can be considered as a 1D photonic Floquet topological insulator. Both the linear and zero dispersion relations support localization of light propagating through the lattice, and so does the edge state. Based on the topologically protected edge state, we propose a structure that realizes an optical switch with high efficiency.

It is worth mentioning that similar topics were investigated previously^{26–29}, however in this Letter we mainly focus on the transport properties of the edge state and also provide a realizable model.

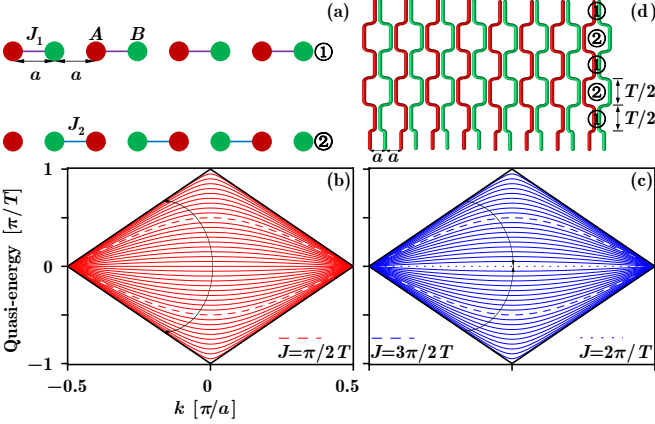


FIG. 1. (a) One-dimensional periodically driven Shockley system with two nonequal sites. Dynamics is divided into two steps of equal frequency, by assuming that the hopping only happens between two sites connected by a bond, with the hopping strengths J_1 and J_2 . (b) and (c) Quasi-energies in the first Brillouin zone under the periodic boundary condition. The hopping strength J is changing from 0 to π/T (b) and from π/T to $2\pi/T$ (c), as indicated by the curved arrows. (d) Schematic sketch of the photonic waveguide system that can mimic the model in (a).

The time-dependent Hamiltonian of the system can be written as

$$H(t) = \begin{bmatrix} c_A^\dagger & c_B^\dagger \end{bmatrix} H(k, t) \begin{bmatrix} c_A \\ c_B \end{bmatrix}, \quad (1)$$

with

$$H(k, t) = - \sum_{n=1}^2 \begin{bmatrix} 0 & J_n \exp(\pm iak) \\ J_n \exp(\mp iak) & 0 \end{bmatrix}, \quad (2)$$

where a is a constant that represents the distance between two adjacent sites, and $c_{A(B)}^\dagger$ is the creation operator for the Bloch state on sublattice $A(B)$. According to Fig. 1(a), the first Brillouin zone is $k \in [-\pi/2a, \pi/2a]$. Thus, the bulk evolution operator over one period is

$$U(T) = \exp(-iH_2T/2) \exp(-iH_1T/2) \quad (3)$$

$$= \begin{bmatrix} \cot^2(JT/2) - \exp(2iak) & 2i \cos(ak) \cot(JT/2) \\ 2i \cos(ak) \cot(JT/2) & \cot^2(JT/2) - \exp(-2iak) \end{bmatrix},$$

from which one finds that the hopping strength J is periodic, with the period $2\pi/T$. This means that one

will obtain the same results for $J \in [0, \pi/T]$ and $J \in [\pi/T, 2\pi/T]$. In Figs. 1(b) and 1(c), we show the quasi-energies under the periodic boundary condition in the first Brillouin zone, but with the hopping strength J changing in $[0, \pi/T]$ and $[\pi/T, 2\pi/T]$, respectively. Clearly, one finds that they are practically the same. In addition, one finds that the quasi-energy changes linearly in the first Brillouin zone if $J = \pi/T$, and there is no diffraction if $J = 2\pi/T$ (the quasi-energy is always 0). Along similar lines, the linear dispersion relation is also reported in non-Hermitian systems^{30,31}.

To investigate transport properties of the model, a waveguide array based on the lattice structure is suggested in Fig. 1(d), the distance between two adjacent waveguides (the lattice sites) is changing so as to adjust for the periodic coupling. Now, the propagation distance z acts as “time”, and the period T is a length. Such a lattice can be fabricated by using the femto-second laser writing technique³² that is frequently employed lately^{13,23,33–35}. We are aware that a similar structure was adopted to investigate the discrete quantum walk^{36,37} and parity-time symmetry^{38–40}, however the physical mechanism here is quite different — it is a one-dimensional case^{16,41}. The behavior of the system crucially depends on the transverse boundary conditions.

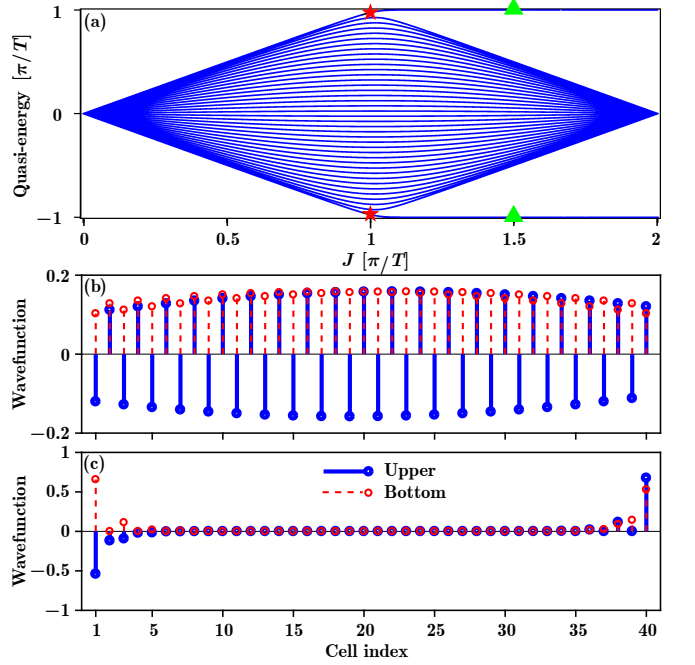


FIG. 2. (a) Quasi-energy changing with the hopping strength under the open boundary condition. (b) and (c) Wavefunctions corresponding to the quasi-energies marked by stars ($J = \pi/T$) and triangles ($J = 1.5\pi/T$) in (a). In the calculation, 40 sites are considered.

When the system is under the open boundary condition, the corresponding quasi-energies (See the Appendix for details of the calculation.) are displayed in Fig. 2(a). Different from the case with the periodic boundary con-

dition, the quasi-energies are not periodic with the coupling strength. When the coupling strength is bigger than π/T , an edge state emerges. In other words, a topological phase transition occurs with the increasing coupling strength. We show the wavefunctions in Figs. 2(b) and 2(c) that correspond to the quasi-energies marked by stars and triangles in Fig. 2(a). In comparison with the case in Fig. 2(b), one clearly finds that the wavefunction is mainly located on the boundary sites in Fig. 2(c), which demonstrates the existence of an edge state. In addition, one finds that the wavefunctions in the upper edge state are odd, while those in the lower edge state are even. We should mention that the wavefunction shown in Fig. 2(c) is gauge dependent, but it still makes sense as an indication of the existence of edge states.

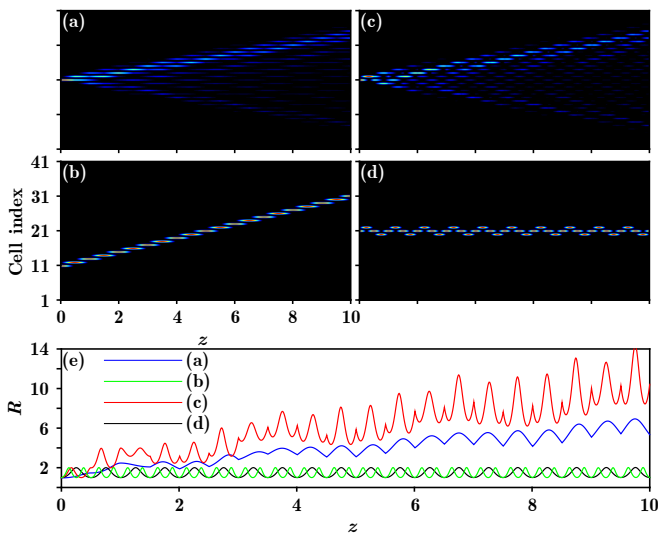


FIG. 3. Propagation dynamics in the waveguide array under the periodic boundary condition when only one site A is excited. (a) $J = 0.5\pi/T$, (b) $J = \pi/T$, (c) $J = 1.5\pi/T$, and (d) $J = 2\pi/T$. (e) The participation ratio during propagation. The ratio is normalized to 1 at the initial place. Parameters: $a = 1$ and $T = 1$. Input Gaussian beam: $\exp[-16 \ln 2 (x - x_A)^2]$ with x_A the position of the site A .

We investigate transport properties of the structure by checking the beam propagation in it. First, we focus on the propagation under the periodic boundary condition (See the Appendix for details of the calculation.), as shown in Fig. 3. We select the coupling strength to be $J = 0.5\pi/T$, $J = \pi/T$, $J = 1.5\pi/T$ and $J = 2\pi/T$, and display the results in Figs. 3(a)-3(d), respectively. Since the quasi-energies for $J = 0.5\pi/T$ and $J = 1.5\pi/T$ are almost the same [the dashed curves in Figs. 1(b) and 1(c)], the propagation in Figs. 3(a) and 3(c) is quite similar — both exhibit discrete diffraction. For $J = \pi/T$ the quasi-energy is linear and the propagation in Fig. 3(b) is along an oblique straight trajectory without diffraction. One can calculate that the slope of the quasi-energy is 2, so the transverse shift of the beam is 20 in a propagation distance of 10, i.e., the numerical simu-

lation completely agrees with the theoretical prediction. It is worth mentioning that such a property can be utilized to achieve light rectification^{42,43}. Whereas for the case with $J = 2\pi/T$, the quasi-energy is zero throughout the first Brillouin zone, as presented by the dotted line in Fig. 1(c), so the corresponding mode (the “zero-energy” state) will be strongly localized during propagation. However, such a zero-energy state is not exactly the same as in the case $J = 0$, which is completely localized at the excited site; the energy will be exchanged among the excited site and its two adjacent sites due to the coupling, as shown in Fig. 3(d).

We would like to emphasize that the localization seen in Figs. 3(b) and 3(d) happens because of the topology, which leads to the linear or zero diffraction. Such topologically enhanced localization is always stable theoretically and has a much higher efficiency than the localization due to the nonlinearity (e.g., discrete solitons). In Fig. 3(e), we display the participation ratio $R = (\int |\psi|^2 dx)^2 / \int |\psi|^4 dx$, with ψ being the transverse envelope of the beam at the site, which measures the localization of light during propagation. The difference between the ratios in Figs. 3(a) and 3(c) is due to the coupling strength that affects the beam intensity at each site. Actually, the results shown in Figs. 3(a) and 3(c) may change with different inputs, but the variation trend that indicates the discrete diffraction remains the same. In comparison with the cases in Figs. 3(a) and 3(c), the light beams in Figs. 3(b) and 3(d) are indeed well localized, because R only changes between 1 and 2.

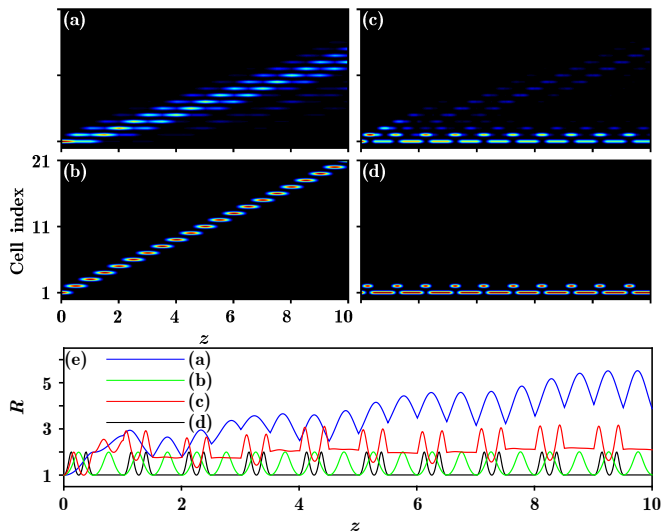


FIG. 4. Same as Fig. 3, but under the open boundary condition, when the boundary site A is excited.

After discussing the case of the system under the periodic boundary condition, we now turn to the case under an open boundary condition. As shown in Fig. 2(a), there will be edge states with the increasing coupling strength. Therefore, light that excites the edge state mode will be localized during propagation. Correspond-

ing to Fig. 3, in Fig. 4 we display light propagation in the lattice under an open boundary condition (See the Appendix for details of the calculation.), when only the boundary site A is excited. Since there is no edge state for the case $J = 0.5\pi/T$, the beam will diffract into the bulk during propagation, as in Fig. 4(a). If $J = \pi/T$, the edge state is still not built up, so it will diffract into the bulk. However, as shown in Fig. 4(b), the propagation dynamics unexpectedly looks the same as in Fig. 3(b). The reason is that the beam does not “feel” the boundary and it always deflects along a certain direction, due to the linear dispersion relation at $J = \pi/T$. One may prepare an input that propagates in the opposite direction, but it will ultimately reflect at the boundary during propagation. Since the light beam is not distorted during propagation, the structure represents a good choice for guiding light that would propagate along a zigzag trajectory⁴⁴.

When the coupling strength increases to $J = 1.5\pi/T$, the edge state will play a role in localization, as in Fig. 4(c). One has to bear in mind that the input beam may also excite the bulk mode, so that a fraction of light may diffract into the bulk. By further increasing the coupling strength to $J = 2\pi/T$, only the edge state will remain in the end. As a result, one obtains the optimum localization, as shown in Fig. 4(d). Again, we display the corresponding participation ratio in Fig. 4(e), from which one finds that the localization due to the edge state is quite pronounced. Also, the participation ratios in Figs. 3(b) and 4(b) are the same (the green curves).

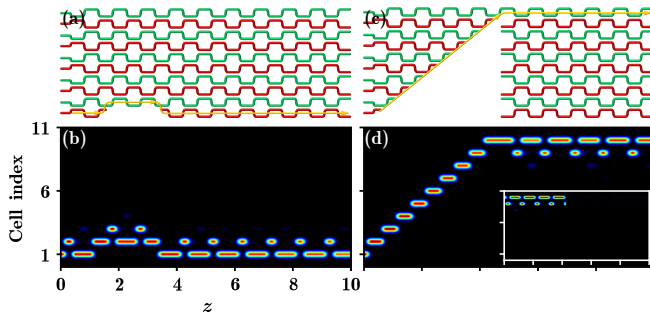


FIG. 5. (a) Periodically driven system with a defect on the boundary. Yellow curves with arrows indicate the predicted propagation direction. (b) The corresponding propagation of light. (c) and (d) Same as (a) and (b), but for the system with successive defects on the boundary. Inset in (d) shows the beam propagation when the upper boundary site B is excited. The coupling strength is $J = 1.8\pi/T$.

We would like to point out that the edge state is topologically protected, and so is the localization. To check such a protection, we deliberately remove the boundary site A in two periods (from $5T/4$ to $13T/4$), to make a defect on the boundary, as shown in Fig. 5(a). If the topological protection works, the light beam will propagate along the trajectory indicated by the yellow curve with an arrow. The corresponding numerical simulation of the propagation is exhibited in Fig. 5(b), from which

one infers that the light beam indeed propagates by bypassing the defect, without being reflected into the bulk.

Furthermore, if one successively introduces defects in the waveguide arrays and considers the topological protection at the same time, as in the structure shown in Fig. 5(c), the light beam may propagate along the yellow curve if the boundary site A is excited. It turns out that the light beam will jump from one boundary to the other, and the numerical simulation in Fig. 5(d) confirms that prediction. On the other hand, if the upper boundary site B is excited, the propagation will be blocked at the exchange point. The inset in Fig. 5(d) elucidates the situation. Clearly, the system described in Fig. 5 can serve as an optical switch. To evaluate the efficiency of the optical switch, we define the ratio $10\log_{10} \frac{\max\{I_A\}}{\max\{I_B\}}$, where $I_{A(B)}$ means the output beam intensity when boundary site $A(B)$ is excited⁴⁵. One finds that the ratio is 4.3 dB for $J = 1.6\pi/T$, 15.3 dB for $J = 1.8\pi/T$, and 25.3 dB for $J = 1.9\pi/T$, which increases sharply with the coupling strength. We believe that our design is highly efficient and easy to realize experimentally.

In summary, we have investigated the topologically enhanced localization in the one-dimensional periodically driven system based on the modified Shockley model. Under the periodic boundary condition, the localization is induced by the zero-energy state, which greatly depends on the coupling strength. Whereas under the open boundary condition, the localization is due to the edge state, which emerges gradually with the increase of the coupling strength. The localization due to the edge state is topologically protected and immune to defects. Finally, a kind of optical switch based on the topological protection is developed. Our numerical simulations demonstrate that the efficiency of such an optical switch can be higher than 20 dB.

ACKNOWLEDGMENTS

This work was supported by China Postdoctoral Science Foundation (2016M600777, 2016M600776, 2016M590935), the National Natural Science Foundation of China (11474228, 61605154), and Qatar National Research Fund (NPRP 6-021-1-005, 8-028-1-001).

¹T. Oka and H. Aoki, “Photovoltaic Hall effect in graphene,” *Phys. Rev. B* **79**, 081406 (2009).

²T. Kitagawa, E. Berg, M. Rudner, and E. Demler, “Topological characterization of periodically driven quantum systems,” *Phys. Rev. B* **82**, 235114 (2010).

³N. H. Lindner, G. Refael, and V. Galitski, “Floquet topological insulator in semiconductor quantum wells,” *Nat. Phys.* **7**, 490–495 (2011).

⁴M. S. Rudner, N. H. Lindner, E. Berg, and M. Levin, “Anomalous edge states and the bulk-edge correspondence for periodically driven two-dimensional systems,” *Phys. Rev. X* **3**, 031005 (2013).

⁵A. Gómez-León and G. Platero, “Floquet-Bloch theory and topology in periodically driven lattices,” *Phys. Rev. Lett.* **110**, 200403 (2013).

- ⁶N. Goldman and J. Dalibard, “Periodically driven quantum systems: Effective hamiltonians and engineered gauge fields,” *Phys. Rev. X* **4**, 031027 (2014).
- ⁷J. K. Asboth and J. M. Edge, “Edge-state-enhanced transport in a two-dimensional quantum walk,” *Phys. Rev. A* **91**, 022324 (2015).
- ⁸T.-S. Xiong, J. Gong, and J.-H. An, “Towards large-Chern-number topological phases by periodic quenching,” *Phys. Rev. B* **93**, 184306 (2016).
- ⁹P. Titum, E. Berg, M. S. Rudner, G. Refael, and N. H. Lindner, “Anomalous Floquet-Anderson insulator as a nonadiabatic quantized charge pump,” *Phys. Rev. X* **6**, 021013 (2016).
- ¹⁰Z. Yu and S. Fan, “Complete optical isolation created by indirect interband photonic transitions,” *Nat. Photon.* **3**, 91–94 (2009).
- ¹¹K. Fang, Z. Yu, and S. Fan, “Realizing effective magnetic field for photons by controlling the phase of dynamic modulation,” *Nat. Photon.* **6**, 782–787 (2012).
- ¹²T. Kitagawa, M. A. Broome, A. Fedrizzi, M. S. Rudner, E. Berg, I. Kassal, A. Aspuru-Guzik, E. Demler, and A. G. White, “Observation of topologically protected bound states in photonic quantum walks,” *Nat. Commun.* **3**, 882 (2012).
- ¹³M. C. Rechtsman, J. M. Zeuner, Y. Plotnik, Y. Lumer, D. Podolsky, F. Dreisow, S. Nolte, M. Segev, and A. Szameit, “Photonic Floquet topological insulators,” *Nature* **496**, 196–200 (2013).
- ¹⁴D. Leykam, M. C. Rechtsman, and Y. D. Chong, “Anomalous topological phases and unpaired Dirac cones in photonic Floquet topological insulators,” *Phys. Rev. Lett.* **117**, 013902 (2016).
- ¹⁵D. Leykam and Y. D. Chong, “Edge solitons in nonlinear-photonic topological insulators,” *Phys. Rev. Lett.* **117**, 143901 (2016).
- ¹⁶L. J. Maczewsky, J. M. Zeuner, S. Nolte, and A. Szameit, “Observation of photonic anomalous Floquet topological insulators,” *Nat. Commun.* **8**, 13756 (2017).
- ¹⁷J. H. Shirley, “Solution of the Schrödinger equation with a hamiltonian periodic in time,” *Phys. Rev.* **138**, B979–B987 (1965).
- ¹⁸H. Sambe, “Steady states and quasienergies of a quantum-mechanical system in an oscillating field,” *Phys. Rev. A* **7**, 2203–2213 (1973).
- ¹⁹L. Lu, J. D. Joannopoulos, and M. Soljačić, “Topological photonics,” *Nat. Photon.* **8**, 821–829 (2014).
- ²⁰A. B. Khanikaev, S. H. Mousavi, W.-K. Tse, M. Kargarian, A. H. MacDonald, and G. Shvets, “Photonic topological insulators,” *Nat. Mater.* **12**, 233–239 (2012).
- ²¹G. Q. Liang and Y. D. Chong, “Optical resonator analog of a two-dimensional topological insulator,” *Phys. Rev. Lett.* **110**, 203904 (2013).
- ²²W.-J. Chen, S.-J. Jiang, X.-D. Chen, B. Zhu, L. Zhou, J.-W. Dong, and C. T. Chan, “Experimental realization of photonic topological insulator in a uniaxial metacrystal waveguide,” *Nat. Commun.* **5**, 5782 (2014).
- ²³Y. Plotnik, M. C. Rechtsman, D. Song, M. Heinrich, J. M. Zeuner, S. Nolte, Y. Lumer, N. Malkova, J. Xu, A. Szameit, Z. Chen, and M. Segev, “Observation of unconventional edge states in ‘photonic graphene,’” *Nat. Mater.* **13**, 57–62 (2014).
- ²⁴S. S. Pershoguba and V. M. Yakovenko, “Shockley model description of surface states in topological insulators,” *Phys. Rev. B* **86**, 075304 (2012).
- ²⁵J. K. Asbóth, L. Oroszlány, and A. Pályi, “The Su-Schrieffer-Heeger (ssh) model,” in *A Short Course on Topological Insulators: Band Structure and Edge States in One and Two Dimensions* (Springer, Cham, 2016) pp. 1–22.
- ²⁶M. Thakurathi, A. A. Patel, D. Sen, and A. Dutta, “Floquet generation of Majorana end modes and topological invariants,” *Phys. Rev. B* **88**, 155133 (2013).
- ²⁷J. K. Asbóth, B. Tarasinski, and P. Delplace, “Chiral symmetry and bulk-boundary correspondence in periodically driven one-dimensional systems,” *Phys. Rev. B* **90**, 125143 (2014).
- ²⁸V. Dal Lago, M. Atala, and L. E. F. Foa Torres, “Floquet topological transitions in a driven one-dimensional topological insulator,” *Phys. Rev. A* **92**, 023624 (2015).
- ²⁹K. I. Seetharam, C.-E. Bardyn, N. H. Lindner, M. S. Rudner, and G. Refael, “Controlled population of Floquet-Bloch states via coupling to Bose and Fermi baths,” *Phys. Rev. X* **5**, 041050 (2015).
- ³⁰G. Della Valle and S. Longhi, “Spectral and transport properties of time-periodic \mathcal{PT} -symmetric tight-binding lattices,” *Phys. Rev. A* **87**, 022119 (2013).
- ³¹Y. Q. Zhang, H. Zhong, M. R. Belić, Y. Zhu, W. P. Zhong, Y. P. Zhang, D. N. Christodoulides, and M. Xiao, “ \mathcal{PT} symmetry in a fractional Schrödinger equation,” *Laser Photon. Rev.* **10**, 526–531 (2016).
- ³²A. Szameit and S. Nolte, “Discrete optics in femtosecond-laser-written photonic structures,” *J. Phys. B: At. Mol. Opt. Phys.* **43**, 163001 (2010).
- ³³R. A. Vicencio, C. Cantillano, L. Morales-Inostroza, B. Real, C. Mejía-Cortés, S. Weimann, A. Szameit, and M. I. Molina, “Observation of localized states in Lieb photonic lattices,” *Phys. Rev. Lett.* **114**, 245503 (2015).
- ³⁴S. Mukherjee, A. Spracklen, D. Choudhury, N. Goldman, P. Öhberg, E. Andersson, and R. R. Thomson, “Observation of a localized flat-band state in a photonic Lieb lattice,” *Phys. Rev. Lett.* **114**, 245504 (2015).
- ³⁵F. Diebel, D. Leykam, S. Kroesen, C. Denz, and A. S. Desyatnikov, “Conical diffraction and composite Lieb bosons in photonic lattices,” *Phys. Rev. Lett.* **116**, 183902 (2016).
- ³⁶M. A. Broome, A. Fedrizzi, B. P. Lanyon, I. Kassal, A. Aspuru-Guzik, and A. G. White, “Discrete single-photon quantum walks with tunable decoherence,” *Phys. Rev. Lett.* **104**, 153602 (2010).
- ³⁷L. Sansoni, F. Sciarrino, G. Vallone, P. Mataloni, A. Crespi, R. Ramponi, and R. Osellame, “Two-particle Bosonic-Fermionic quantum walk via integrated photonics,” *Phys. Rev. Lett.* **108**, 010502 (2012).
- ³⁸A. Regensburger, C. Bersch, M.-A. Miri, G. Onishchukov, D. N. Christodoulides, and U. Peschel, “Parity-time synthetic photonic lattices,” *Nature* **488**, 167–171 (2012).
- ³⁹A. Regensburger, M.-A. Miri, C. Bersch, J. Näger, G. Onishchukov, D. N. Christodoulides, and U. Peschel, “Observation of defect states in \mathcal{PT} -symmetric optical lattices,” *Phys. Rev. Lett.* **110**, 223902 (2013).
- ⁴⁰M. Wimmer, A. Regensburger, M.-A. Miri, C. Bersch, D. N. Christodoulides, and U. Peschel, “Observation of optical solitons in \mathcal{PT} -symmetric lattices,” *Nat. Commun.* **6**, 7782 (2015).
- ⁴¹S. Mukherjee, A. Spracklen, M. Valiente, E. Andersson, P. Öhberg, N. Goldman, and R. R. Thomson, “Experimental observation of anomalous topological edge modes in a slowly driven photonic lattice,” *Nat. Commun.* **8**, 13918 (2017).
- ⁴²S. Longhi, “Rectification of light refraction in curved waveguide arrays,” *Opt. Lett.* **34**, 458–460 (2009).
- ⁴³F. Dreisow, Y. V. Kartashov, M. Heinrich, V. A. Vysloukh, A. Tnnermann, S. Nolte, L. Torner, S. Longhi, and A. Szameit, “Spatial light rectification in an optical waveguide lattice,” *EPL (Europhys. Lett.)* **101**, 44002 (2013).
- ⁴⁴Y. Q. Zhang, X. Liu, M. R. Belić, W. P. Zhong, Y. P. Zhang, and M. Xiao, “Propagation dynamics of a light beam in a fractional Schrödinger equation,” *Phys. Rev. Lett.* **115**, 180403 (2015).
- ⁴⁵L. Chang, X. Jiang, S. Hua, C. Yang, J. Wen, L. Jiang, G. Li, G. Wang, and M. Xiao, “Parity-time symmetry and variable optical isolation in active-passive-coupled microresonators,” *Nat. Photon.* **8**, 524–529 (2014).

Appendix A: Band structure of the periodically driven 1D system with open boundary condition

We assume there are 4 sites for the periodically driven 1D system with open boundary condition as shown in Fig. 6.

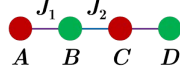


FIG. 6. The periodically driven 1D system with open boundary condition.

The Hamiltonian of the system can be written as

$$H = J_1 A^* B \exp(ik_x) + J_1 B^* A \exp(-ik_x) + J_2 B^* C \exp(ik_x) + J_2 C^* B \exp(-ik_x) + J_1 C^* D \exp(ik_x) + J_1 D^* C \exp(-ik_x). \quad (\text{A1})$$

Writing Eq. (A1) into matrix format, as

$$H = \begin{bmatrix} A^* & B^* & C^* & D^* \end{bmatrix} \mathcal{H} \begin{bmatrix} A \\ B \\ C \\ D \end{bmatrix}, \quad (\text{A2})$$

where the Hamiltonian kernel is

$$\mathcal{H} = \exp(ik_x) \times \begin{bmatrix} 0 & J_1 & 0 & 0 \\ J_1 \exp(-i2ak_x) & 0 & J_2 & 0 \\ 0 & J_2 \exp(-i2ak_x) & 0 & J_1 \\ 0 & 0 & J_1 \exp(-i2ak_x) & 0 \end{bmatrix}.$$

The eigenvalue of \mathcal{H} is the band structure we are looking for. We assume the 1D system has 40 sites, and the band structure with different J is displayed in Fig. 7. The top panel shows the case with $J = 0.5\pi/T$, the middle case with $J = \pi/T$, and the bottom panel with $J = 1.5\pi/T$. One can find that the edge state emerges in Fig. 7(c).

Appendix B: Propagation of light in the waveguide arrays

Propagation of light in the waveguide array under the periodic boundary condition can be depicted by the coupled equations

$$\begin{aligned} i \frac{dA}{dz} &= [J_1 \exp(ik_x) + J_2 \exp(-ik_x)] B, \\ i \frac{dB}{dz} &= [J_1 \exp(-ik_x) + J_2 \exp(ik_x)] A. \end{aligned} \quad (\text{B1})$$

Equation (B1) can be numerically solved by using the 4th order Runge-Kutta method. For static system, the coupling strength $J_1 = J_2 = J$; if light is launched into

one site, discrete diffraction will be observed, as shown in Fig. 8(a). For the periodically driven system, the propagation is shown in Fig. 8(b), which is also Fig. 3(a) in the main text.

While for the case under the open boundary condition, we also take Fig. 6 for example with sites A and D being

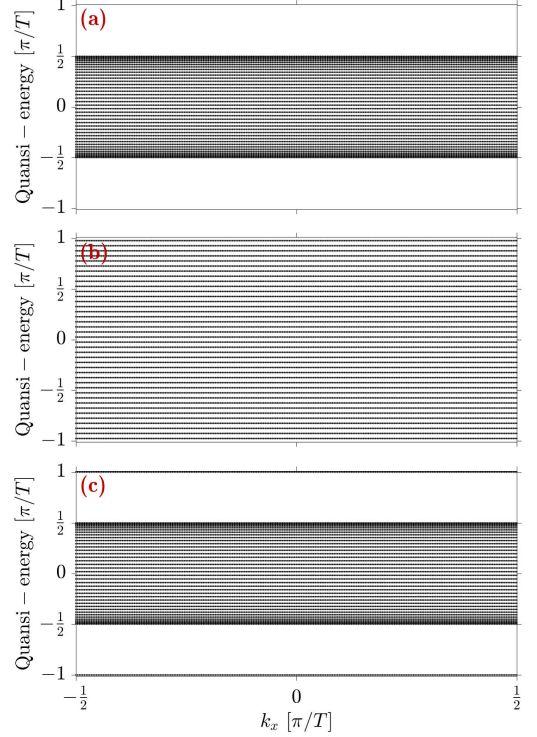


FIG. 7. Band structure of the periodically driven 1D system with $J = 0.5\pi/T$ (a), $J = \pi/T$ (b), and $J = 1.5\pi/T$ (c).

the boundary sites, the governing equation is

$$\begin{aligned} i \frac{dA}{dz} &= J_1 \exp(ik_x) B, \\ i \frac{dB}{dz} &= J_1 \exp(-ik_x) A + J_2 \exp(ik_x) C, \\ i \frac{dC}{dz} &= J_2 \exp(-ik_x) B + J_1 \exp(ik_x) D, \\ i \frac{dD}{dz} &= J_1 \exp(-ik_x) C. \end{aligned} \quad (\text{B2})$$

Clearly, Eq. (B2) can be also numerically solved by using the 4th order Runge-Kutta method. We also take 40 sites for example, and the numerical results are displayed in Figs. 8(c) and 8(d).

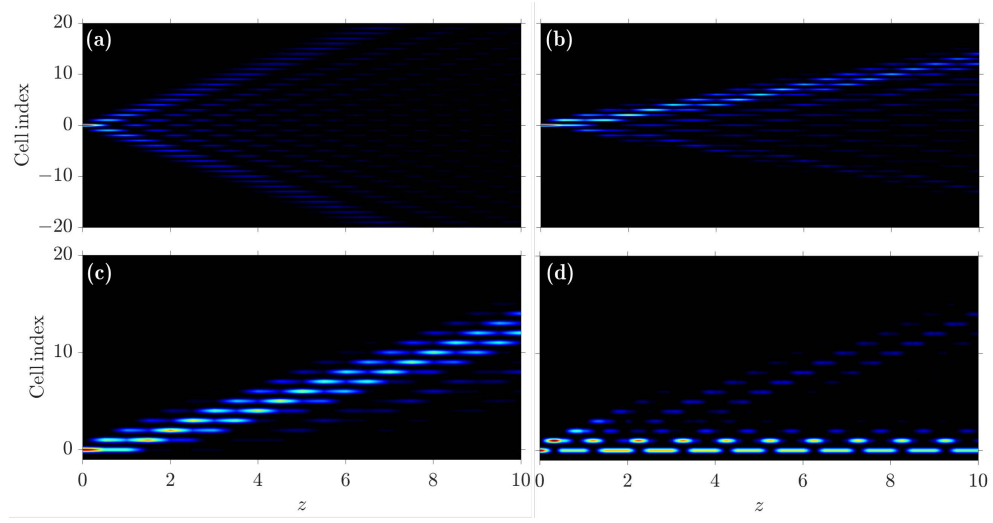


FIG. 8. Propagation of light in the 1D system. (a) The system under the periodic condition is static with $J_1 = J_2 = 0.5\pi/T$. (b) The system under the periodic condition is periodically driven with $(J_1, J_2) = (0.5\pi/T, 0)$ and $(J_1, J_2) = (0, 0.5\pi/T)$ periodically. (c) and (d) The system under the open condition is periodically driven with $J = 0.5\pi/T$ and $J = 1.5\pi/T$.